PERIÓDICO TCHÊ QUÍMICA
ARTIGO ORIGINAL

ESTUDO DA SITUAÇÃO DE RADIAÇÃO EM MOSCOU POR MEIO DA PESQUISA DOS ORGANISMOS ELASTOPLÁSTICOS NO FLUXO DE NÊUTRONS, CONSIDERANDO OS EFEITOS DO CALOR

STUDY OF THE RADIATION SITUATION IN MOSCOW BY INVESTIGATING ELASTOPLASTIC BODIES IN A NEUTRON FLUX TAKING INTO ACCOUNT THERMAL EFFECTS

ИЗУЧЕНИЕ РАДИАЦИОННОЙ ОБСТАНОВКИ В МОСКВЕ ПУТЕМ ИССЛЕДОВАНИЯ УПРУГОПЛАСТИЧЕСКИХ ТЕЛ В НЕЙТРОННОМ ПОТОКЕ С УЧЕТОМ ТЕПЛОВЫХ ЭФФЕКТОВ

PRONINA, Polina F.[1*]; TUSHAVINA, Olga V.[2]; STAROVOITOV, Eduard I.[3];

[1] Moscow Aviation Institute (National Research University), Institute of Aerospace, Department of Managing Exploitation of Space-Rocket Systems, 4 Volokolamskoe Highway, zip code 125993, Moscow – Russian Federation

[2] Moscow Aviation Institute (National Research University), Institute of Aerospace, 4 Volokolamskoe Highway, zip code 125993, Moscow – Russian Federation

[3] Belarusian State University of Transport, Department of Building Mechanics, 34 Kirov Str., zip code 246653, Gomel – Republic of Belarus

** Correspondence author*
e-mail: pronina-p19.94@yandex.ru

Received 21 April 2020; received in revised form 09 June 2020; accepted 19 June 2020

RESUMO

Este artigo examina o estudo do nível de radiação de fundo em Moscou e seu impacto no meio ambiente. Para identificar os efeitos radiológicos nas condições de vida, foi realizado um estudo sobre os efeitos dos nêutrons rápidos na infraestrutura e nos objetos biológicos. Foram consideradas as organizações de pesquisa em larga escala que realizam desenvolvimento tecnológico, pesquisa científica e material utilizando materiais nucleares na cidade de Moscou e na região. O sistema de monitoramento de radiação do meio ambiente, cobrindo uma área de mais de 1091 km^2, foi examinado em detalhes. Uma pesquisa radioecológica realizada nos distritos administrativos Troitskiy e Novo-Moscovskiy foi analisada para identificar e descrever a situação da radiação. A análise da radiação de fundo em Moscou mostra que os valores dos parâmetros controlados da poluição radioativa de objetos ambientais estão dentro das flutuações de longo prazo do fundo tecnogênico da capital. Nesse caso, surgem vários efeitos térmicos, causados pela exposição à radiação de sólidos. O estudo da infraestrutura e dos objetos biológicos é realizado com base na determinação de efeitos, que resultam em mudança das características elásticas e especialmente plásticas das substâncias expostas à irradiação de nêutrons e aos efeitos térmicos. Nesse caso, os principais fatores importantes são o endurecimento por radiação do material (aumento do limite de extensão gradual) e o inchaço induzido por radiação (aumento da deformação volumétrica).

Palavras-chave: *monitoramento radioecológico, dose de radiação absorvida, taxa de dose de exposição, atividade volumétrica de equilíbrio equivalente, carga quasistática.*

ABSTRACT

This article discusses the study of the background radiation level in Moscow and its impact on the environment. To identify the radiological impact on living conditions, a study of the effects of fast neutrons on infrastructure and biological objects was made. Large-scale research organizations carrying out technological development, scientific and materials research using nuclear materials in the city of Moscow and the region are considered. A system of environment radiation monitoring, covering an area of more than 1091 km², was examined in detail. A radioecological survey conducted in the Troitsky and Novomoskovsky administrative districts was analyzed to identify and describe the radiation situation. An analysis of background radiation in Moscow

DOI: 10.52571/PTQ.v17.n35.2020.64_PRONINA_pgs_753_764.pdf

shows that the values of the controlled parameters of radioactive pollution of environmental objects are within the long-term fluctuations of the technogenic background of the capital. In this case, various thermal effects arise caused by radiation exposure to solids. The study of infrastructure and biological objects is carried out based on the determination of effects, because of which the elastic and mainly plastic characteristics of substances exposed to neutron irradiation and thermal effects change. Here, the main essential factors are radiation hardening of the material (increase in yield stress) and radiation swelling (increase in volumetric strain).

Keywords: *radioecological monitoring, absorbed radiation dose, exposure dose rate, equilibrium equivalent concentration, quasistatic loading.*

АННОТАЦИЯ

В данной статье рассматривается исследование уровня радиационного фона в Москве и воздействие его на окружающую среду. Для выявления радиологического воздействия на условия жизни было проведено исследование воздействия быстрых нейтронов на инфраструктуру и биологические объекты. Рассмотрены крупномасштабные научно-исследовательские организации, выполняющие технологические разработки, научные и материаловедческие исследования с использованием ядерных материалов в городе Москве и области. Была детально рассмотрена система радиационного мониторинга окружающей среды, занимающая площадь более 1091 км^2. Радиоэкологическое обследование, проведенное в Троицком и Ново-Московском административных округах, было проанализировано с целью выявления и описания радиационной обстановки. Анализ фоновой радиации в Москве показывает, что значения контролируемых параметров радиоактивного загрязнения объектов окружающей среды находится в пределах многолетних колебаний техногенного фона столицы. При этом возникают различные тепловые эффекты, которые вызываются радиационным облучением твердых тел. Исследование инфраструктуры и биологических объектов проводится на основе определения эффектов, в результате которых изменяются упругие и особенно пластические характеристики веществ, подверженных воздействию нейтронному облучению и тепловому воздействию. Здесь основными важными факторами являются радиационное упрочнение материала (увеличение предела текучести) и радиационное разбухание (увеличение объемной деформации).

Ключевые слова: *радиоэкологический мониторинг, поглощённая доза обучения, мощность экспозиционной дозы, эквивалентная равновесная объемная активность, квазистатические нагружения.*

1. INTRODUCTION

In recent years, the radiation situation on Earth has undergone significant changes. As a result of numerous ground atomic testings, the radioactivity build-up occurred (Sean Hubar, 2017; Cuttler, 2019; Huang *et al*., 2020; Inoue *et al*., 2020). 12.5 tons of fission products were thrown into the biosphere (Pant *et al*., 2018; Saha *et al*., 2019; Orlov *et al*., 2003; Skvortsov *et al*., 2014; Litvishko *et al*., 2020; Mietelski and Povinec, 2020). All explosions from atmospheric nuclear tests changed the equilibrium content of tritium by almost 100 times and by 2.6% to equilibrium content of carbon-14, which led to an excess of the natural background radiation by 2% (Aleikin *et al*., 2019; Pivovarov and Mikhalev, 2004; Chubirko *et al*., 2019; Tushavina *et al*., 2019; Yakovlev *et al*., 2020; Dridi *et al*., 2020).

The accident at the Chernobyl nuclear power plant led to the release of 15 tons of radioactive substances into the biosphere. However, the danger of nuclear fuel cycle facilities is not only in the field of accidents and disasters (Rabi *et al*., 2017; Ali *et al*., 2018; Renaud *et al*., 2020). Even without them, about 250 radioactive isotopes fall into the environment as a result of the nuclear facilities operation (Kuznetsov, 2003; Tushavina *et al*., 2019; Topchy, 2018; Kuznetsov *et al*., 2019). One of the most acute problems in the world is the problem of radioactive waste (Prister *et al*., 2018; Umbetov *et al*., 2016; Yudaev *et al*., 2019; Carlberg *et al*., 2019; Taleyarkhan, 2020). In 1994, 554 “lost” or unauthorized dumping sites of ionizing radiation sources in Moscow, St. Petersburg, Bratsk, Volgograd, and hundreds in other territories were identified in Russia. Thus, the highest levels of pollution were found in St. Petersburg (> 40 R/h) and Cherepovets (> 2 R/h) (Zverev, 2010; Okhrimenko *et al*., 2017; Shugurov and Knyazyuk, 2018; Umbetov *et al*., 2017; Trotsenko *et al*., 2019).

On the territory of Moscow, in the course of scrupulous surveys carried out after the Chernobyl events, up to 80 places of unregistered “burial

sites" of used radionuclides were found. In general, over ten years after the accident, up to 600 "mortuaries" of this kind were liquidated (Kuznetsov, 2003; Mikayilova, 2017). Moscow is the only capital of the world where on December 25, 1946, the first reactor on the European continent was launched. The city also has large research organizations that carry out technological developments, scientific and materials research using nuclear materials. This is the Russian Scientific Centre "Kurchatov Institute" since 1943, the State Scientific Center High-Tech Research Institute of Inorganic Materials named after Academician A.A. Bochvar since 1945, ARRICT since 1951. Therefore, our work aimed to examine the city of Moscow to determine the radiation situation, as well as to study the behavior of various bodies and biological objects under the influence of neutron and thermal radiation.

The study of infrastructure and biological objects is carried out based on the determination of effects, as a result of which the elastic and mainly plastic characteristics of substances exposed to neutron irradiation and thermal effects change (Liu and Wu, 2018; Bulavin *et al*., 2018; Lazarenko *et al*., 2018; Forkapić *et al*., 2019; Chao *et al*., 2020). Here, the main essential factors are radiation hardening of the material (increase in yield stress) and radiation swelling (increase in volumetric strain).

In this work, the radiation exposure to solids, which is accompanied by numerous thermal effects, as a result of which additional volumetric strain θ1 arises in them, and elastic and mainly plastic characteristics of the substance change was studied.

2. MATERIALS AND METHODS

The system of radioecological monitoring in Moscow covers the entire territory of the city (> 1091 km²) and consists of stationary and mobile means of monitoring, the central laboratory complex, and the information-analytical center. Because of the research, a methodology for studying the stress-strain state of elastoplastic bodies and biological objects under cyclic loading in neutron and heat fluxes is proposed. To study the radiation exposure of solid materials, which is accompanied by numerous thermal effects, were chosen isotropic materials based on aluminum and steel. It was believed that neutrons fall with the same average energy and intensity. The temperature field was assumed to be constant. The kinematic and dynamic parameters of elastoplastic bodies in a neutron flux, taking into account thermal effects, were determined on the basis of the methods of the dynamic theory of elastoplastic bodies (Taleyarkhan, 2020).

Consider an initial homogeneous isotropic body occupying the half-space z 0. The half-space is affected by the neutron flux and the temperature field (Figure 1). If neutrons with the same average energy and intensity φ0, neutron/(m²sec) are incident on the boundary (z = 0) parallel to the z-axis, then the intensity of the neutron flux reaching the plane z = const will be Equation 1 (Starovoitov *et al*., 2009). The temperature field is assumed to be constant and determined by the function ΔT. The quantity μ in (1) is called the macroscopic cross-section and is of the order of 1/m. For any chemical element, it is calculated by Equation 2 (Starovoitov *et al*., 2009), where σ is the cross-section assigned to one core, n_0 is the number of cores per 1 cm^3, A_0 is the Avogadro's number, ρ is the density, *A* is the atomic weight.

As an example, aluminum σ = 0.21·10^{-24} cm^2, A_0 = 6.022·10^{23} mol^{-1} density ρ = 2.7 g/cm^3, *A* = 27 dalton was considered. Substituting these values in Equation 2, $\mu = 1{,}26\,\text{м}^{-1}$ was obtained. If φ_0 is constant, then by the time *t*, a flux will pass through section *z* (Equation 3). In a rough approximation, it can be assumed that the change in the volume of a substance is directly proportional to the flux I(*z*) and, therefore (Equation 4), where *B* is the experimental constant. Value (Equation 5) gives the total neutron flux per unit surface area of the body. In reactors, φ_0 is of the order of 10^{17}–10^{18} neutrons/(m²sec), and I_0 reaches 10^{23}–10^{27} neutrons/(m²sec), with θ_I being of the order of 0.1. Therefore, depending on the energy of neutrons and the irradiated material, the value of *B* can be of the order of 10^{-28}–10^{-24} m^2/neutron (Starovoitov *et al*., 2009).

The dependences of the elasticity modulus, yield stress and ultimate stress limit, and the entire stress-strain diagram on I_0 for various energies were studied experimentally after irradiation of the samples in atomic reactors. For massive bodies with a flat boundary, the number of neutrons passing at a depth z below this boundary in time *t* is determined by Equation 3. Therefore, the yield stress will be variable in thickness *z*. On the body surface (*z* = 0), the effect of radiation on the plasticity limit σ_y is quite satisfactorily described by the equation of radiation hardening (Equation 6) (Starovoitov *et al*., 2009), where σ_{y0} is the plasticity limit of unirradiated material, where the neutron flux value *I*(*z*) is described by Equation

Erro! Fonte de referência não encontrada.; A, ξ are the constants of the material obtained from the experiment.

3. RESULTS AND DISCUSSION:

Let's consider the process of effects of external forces and radiation flux on a deformable body within the framework of the theory of small elastoplastic strains. Suppose that at the initial moment, a body in a natural state is immediately affected by external forces F_i', R_i' at interface displacement u_{i0}', and at the same time a neutron flux of $I_0 = \varphi_0 t$ is incident on its surface. It is assumed that under such an impact, areas of elastic and plastic strains appear in the body. The change in the elastic moduli due to neutron irradiation was neglected. The stresses, strains, and displacements arising in the body are marked with one stroke at the top.

For example, if for aluminum alloy 356, A = 1.09; m^2/neutron was taken, then satisfaction with known experimental data can be judged by Figure 2. Dark points – experiment, solid line – calculation by equation (6). The corresponding deformation values are denoted by εy0, εy.

In the elastic regions of a solid body, Hooke's law is valid, and the well-known relations between the stress deviators and strain deviators $s_{ij}', э_{ij}'$, and their spherical parts σ', ε' corrected for additional volumetric strain due to the influence of *BI* neutron irradiation and thermal effects ΔT are fulfilled (Equation 7), where *G* is the modulus of elasticity in shear, *K* is the volumetric strain modulus, α is the linear expansion coefficient of the material, ΔT is the temperature change.

For those areas of the solid body where plastic strains appeared, the connection of deviators in the case of simple loading can be represented as (Equation 8), where $f'\left(\varepsilon_u', I, a_k'\right)$ is the plasticity function, which depends on the strain intensity ε_u', the magnitude of the neutron flux *I* and the approximation parameters a_k'.

With a sufficiently fast "instantaneous" application of the power load, the hardening effect of radiation will not have time to affect, and the resulting areas of plastic strain will be the same as without the influence of the neutron flux. Under slow active loading, the outer layers of the body will become hardened over time, and the areas of plastic strain in them may turn out to be less or absent altogether, compared with an unirradiated body. In its effect on elastoplastic bodies, radiation exposure is opposite to thermal, which reduces the yield stress and leads to an increase in plastic strain zones at the same loads (Figure 3).

To relations (Equation 8), differential equations of equilibrium, Cauchy equations, and boundary conditions under the assumption of small deformations was added (Equations 9-10). The comma in the subscript indicates the differentiation operation by the coordinate following it. Changes in the time of external loads and interface displacements occur in such a way that the corresponding loading paths do not belong to the class of substantially complex loads, and radiation hardening and thermal action occur after the forced strain of a solid body.

Let, starting from time t_1, the influence of the neutron flux ceases (φ = 0), and the external forces change in such a way that unloading and subsequent alternating loading with bulk F_i'' and surface forces R_i'' (on S_σ) occur at all points of plastically deformable regions of the body V_p' at the interface displacement ui_0'' (on S_u). The level of exposure to the body remains constant and equal to its value before unloading (Equation 11).

The plasticity limit at points of the body depends on the *z* coordinate and becomes equal to $\sigma_y''(I_1(z))$, that is, it depends on the magnitude of the strain and radiation hardening (Figure 3). Following (Starovoitov *et al*., 2019), one can determine the kinematic and dynamic parameters of elastoplastic bodies in a neutron flux, taking into account the thermal effects. For this, as an example, the problem of repeated radiation-force bending of a three-layer cantilever beam under the influence of a temperature field was considered.

For the three-layer beam, which is asymmetric in thickness, the hypotheses of a broken normal are accepted: Kirchhoff hypothesis is valid in the base layers, the normal remains straight in the filler, does not change its length, but rotates by some additional angle $\psi(x)$. Let the outer base layers of the beam be made of metal and the inner layer (filler) incompressible in thickness – from polymer. The base layers are accepted as elastoplastic, and the filler is nonlinearly elastic. An analytical solution to the corresponding problem of the elasticity theory is given in (Gorshkov *et al*., 2005). The study of thermal processes in various media is described in (Rabinskii and Tushavina, 2019; Rabinskiy and Tushavina, 2019a; Rabinskiy and Tushavina, 2019b; Starovoitov and Leonenko, 2019; Rabinskiy *et al*., 2019; Astapov *et al*., 2019; Antufev *et al*., 2019; Rabinsky and Kuznetsova, 2019; Makarenko and Kuznetsova, 2019).

Let to the outer surface (Equation 12) of the considered three-layer beam, in addition to the distributed power load, $p(x), q(x)$ a neutron flux of density φ_0 is supplied in the direction opposite to the external normal and the temperature field (Figure 4). To describe the deformation of layer materials in a neutron flux, equations of state of type (Equation 8) was used (Equation 13), where $f'^{(k)}$ is the universal function of nonlinearity at loading from a natural state (Equation 14) $\omega'^{(k)}(\varepsilon_u'^{(k)}, I)$ in the base layers, the plasticity function of Ilyushin is used, in the filler – the function of nonlinearity.

In the future, it will be assumed that changes in time of external loads and interface displacements occur in such a way that the corresponding loading paths do not belong to the class of essentially complex loads. Also, the radiation growth in the plasticity limit does not exceed the growth in the strain intensity at the irradiated points of the solid body, which would prevent the formation of plastic strains.

The considered problem of loading from a natural state was solved by the method of linear approximation (Gorshkov *et al*., 2005). In our case, following relations (Equation 14) (under the influence of a neutron flux and a temperature field), the solution was obtained by the same method. As a result, the desired strains are determined by the following recurrence equations (*n* is the approximation number) (Equation 15). Here, $p_\omega'^{(n-1)}$, $h_\omega'^{(n-1)}$, $q_\omega'^{(n-1)}$ additional "external" loads serve as corrections for the plasticity and physical nonlinearity of the materials of the layers under repeated loading and take into account the effect of the neutron flux and temperature. They are taken equal to zero at the first step (*n* = 1), and further calculated by the results of the previous approximation, the fourth-order function $g'^{(n)}(x)$, coefficients $\alpha_1, \alpha_2, \alpha_3, \beta^2, \gamma_1, \gamma_2, \gamma_3$, and linear integral operators $L_2^{-1}, L_3^{-1}, L_4^{-1}$ are defined in (Gorshkov *et al*., 2005). Integration constants $C_1^{(n)}, ..., C_8^{(n)}$ take into account the effects of neutron and heat fluxes. In the case of a *rigid cantilever termination* of the left end of the rod with a free right, satisfying the boundary conditions, was obtained (Equation 16).

With repeated alternating loading, the recurrent solution for quantities with asterisks will be similar (Equation 16) (Equation 17). Numerical results were obtained for a three-layer beam, the layers of which are made of D16T – fluoroplastic – D16T. Relative layer thicknesses: $h_1 = h_2 = 0.03$, c=0.09. The mechanical and radiation parameters of the layer materials included in the equation (16) are given in (Gorshkov *et al*., 2005; Tushavina *et al*., 2019). In addition, it was taken: $B = 10^{-23}$ m^2/neutron, which ensures a volumetric strain of 3–3.5% in the layers of the considered rod, – μ = 1.26 cm for duralumin, and μ = 3.21 cm for fluoroplastic.

Figure 5 shows the change in the deflection $w - a$ along the axis of the three-layer rod under consideration, calculated according to various physical equations of state with cantilever restraint of the left end. Curves with one stroke correspond to loading from the natural state: *1*, *2* – elastic and elastoplastic rods without irradiation, *3* – elastoplastic rods at $\varphi = 10^{18}$ neutron/(m^{2}s) and $\Delta T = 300$ град. With repeated loading, the displacements decrease by 2–3%, both for unirradiated and irradiated rods, which is explained by the cyclic hardening of the material with each change in the sign of the load. On each half-cycle, the conditions of simple loading at small strains are satisfied.

4. CONCLUSIONS:

It is shown that the maximum level of neutron irradiation can cause loosening of the substance, and the heat flux is harmful to biological objects. Calculations show that the impact of the radiation situation slightly affects the stress-strain state of elastoplastic bodies and biological objects. In this case, the action of the temperature field significantly affects the kinematic and static parameters of the objects.

A method for studying the stress-strain state of elastoplastic bodies under cyclic loading of a neutron flux is proposed, which significantly simplifies the solution of a whole class of boundary value problems. The mathematical model presented in the work has restrictions on the maximum level of neutron irradiation, which should not cause loosening of the substance. In this case, on each half-cycle, the conditions of simple loading and deformation must be satisfied.

5. ACKNOWLEDGMENTS:

The work was carried out with the financial support of the state project of the Ministry of Education and Science project code "Modern technologies of experimental and digital modeling and optimization of spacecraft systems parameters", project code FSFF-2020-0016.

6. REFERENCES:

1. Aleikin, V.V., Generalova, V.V., Gromov, A.A., and Kovalenko, O.I. (2019). State primary special standard of the unit of absorbed dose rate of intense photon, electron, and beta radiation for radiation technologies get 2009-2014. *Atmospheric Measurement Techniques, 62*, 587–591. https://doi.org/10.1007/s11018-019-01664-4
2. Ali, M.Y.M., Hanafiah, M.M., and Khan, M.F. (2018). Potential factors that impact the radon level and the prediction of ambient dose equivalent rates of indoor microenvironments. *Science of The Total Environment*, *626*, 1-10.
3. Antufev, B.A., Egorova, O.V., Medvedskii, A.L., and Rabinskiy, L.N. (2019). Dynamics of shell with destructive heat-protective coating under running load. *INCAS Bulletin*, *11*, 7-16. https://doi.org/10.13111/2066-8201.2019.11.S.2.
4. Astapov, A.N., Lifanov, I.P., and Rabinskiy, L.N. (2019). Perspective heat-resistant coating for protection of Cf/SiC composites in air plasma hypersonic flow. *High Temperature*, *57*(5), 744-752.
5. Bulavin, L.A., Alekseev, O.M., Zabashta, Y., and Lazarenko, M.M. (2018). Phase equilibrium, thermodynamic limit, and melting temperature in nanocrystals. *Ukrainian Journal of Physics*, *63*(11), 1036-1040.
6. Carlberg, M., Hedendahl, L., Koppel, T., and Hardell, L. (2019). High ambient radiofrequency radiation in Stockholm city, Sweden. *Oncology Letters, 17*, 1777-1783. https://doi.org/10.3892/ol.2018.9789
7. Chao, N., Yang, H., Liu, Y.-K., Xia, H., and Ayodeji, A. (2020). A local method of characteristics for dose assessment. *Radiation Physics and Chemistry*, *173*, Article 108869.
8. Chubirko, M.I., Klepikov, O.V., Kurolap, S.A., Kuzmichev, M.K., and Studenikina, E.M. (2019). Estimation of the equivalent dose rate of gamma radiation in the open territory of the city of Voronezh. *Radiation Hygiene, 12*(4), 66-71. https://doi.org/10.21514/1998-426X-2019-12-4-66-71
9. Cuttler, J.M. (2019). Evidence of dose threshold for radiation-induced leukemia: absorbed dose and uncertainty. *Dose-Response*. Retrieved from https://journals.sagepub.com/doi/10.1177/1559325818820973.
10. Dridi, W., Daoudi, M., Faraha, K., and Hosni, F. (2020). Monte Carlo validation of dose mapping for the Tunisian Gamma Irradiation Facility using the MCNP6 code. *Radiation Physics and Chemistry*, *173*, Article number 108942.
11. Forkapić, S., Lakatoš, R., Čeliković, I., Bikit Schroeder, K., Mrdja, D., Radolić, V., and Samardžić, S. (2019). Proposal and optimization of method for direct determination of the thoron progeny concentrations and thoron equilibrium. *Radiation Physics and Chemistry*, *159*, 57-63.
12. Gorshkov, A.G., Starovoitov, E.I., and Yarovaya, A.V. (2005). *Mechanics of layered viscoelastic structural elements*. Moscow, Russian Federation: FIZMATLIT.
13. Huang, J., Wang, Q., Qi, Z., Zhou, S., Zhou, M., and Wang, Z. (2020). Lipidomic profiling for serum biomarkers in mice exposed to ionizing radiation. *Dose-Response*. Retrieved from https://journals.sagepub.com/doi/10.1177/1559325820914209.
14. Inoue, K., Sahoo, S.K., Veerasamy, N., Kasahara, Sh. and Fukushi, M. (2020). Distribution patterns of gamma radiation dose rate in the high background radiation area of Odisha, India. *Journal of Radioanalytical and Nuclear Chemistry*, *324*, 1423–1434. https://doi.org/10.1007/s10967-020-07176-8
15. Kuznetsov, V.K., Sanzharova, N.I., Panov, A.V., and Isamov, N.N. (2019). Radioecological monitoring of agroecosystems in the npp vicinity: Methodology and results of investigations. *Medical Radiology and Radiation Safety*, *4*, 25-31.
16. Kuznetsov, V.M. (2003). *Nuclear danger*. Moscow, Russian Federation: Yabloko.
17. Lazarenko, M.M., Alekseev, A.N., Alekseev, S.A., Grabovsky, Y., Lazarenko, M.V., and Hnatiuk, K.I. (2018). Structure and thermal motion of 1-octadecene, confined in the pores of porous silicon. *Molecular Crystals and Liquid Crystals*, *674*(1), 19-30.
18. Litvishko, V., Akhmetova, A., Kodasheva, G., Zhussupova, A., Malikova, R., and Kuralova, A. (2020). Formation of ecological education of the population. *E3S Web of Conferences, 159*, 01009.

19. Liu, R., and Wu, H. (2018, August). *Study on Radiation effects of central cities in Beijing-Tianjin-Hebei region*. Paper presented at the International Conference on Construction and Real Estate Management, Charleston, South Carolina.

20. Makarenko, A.V., and Kuznetsova, E.L. (2019). Energy-efficient actuator for the control system of promising vehicles. *Russian Engineering Research*, *39*(9), 776-779.

21. Mietelski, J.W., and Povinec, P. (2020). Environmental radioactivity aspects of recent nuclear accidents associated with undeclared nuclear activities and suggestion for new monitoring strategies *Journal of Environmental Radioactivity*, *214–215*, Article number 106151.

22. Mikayilova, A.C. (2017). Radioecological monitoring in the Central Zone of Azerbaijan. *Applied Science Reports*, *17*(3). Retrieved from https://ssrn.com/abstract=3200928.

23. Okhrimenko, S.E., Korenkov, I.P., Miklyaev, P.S., Prokhorov, N.I., Verbova, L.F., Orlov, Yu.V., Petrova, T.B., Lashchyonova, T.N., Akopova, N.A., and Kiselev, S.M. (2017). Ranking of the territory of the city of Moscow for potential radon danger. *Hygiene and Sanitation*, *96*(3). Retrieved from https://www.medlit.ru/journalsview/gigsan/view/journal/en/2017/issue-3/2626-ranking-of-the-territory-of-the-city-of-moscow-for-potential-radon-danger/.

24. Orlov, A.M., Skvortsov, A.A., and Litvinenko, O.V. (2003). Bending vibrations of semiconductor wafers with local heat sources. *Technical Physics, 48*(6), 736-741.

25. Pant, P., Kandari, T., Prasad, M., Semwal, P. and Ramola, R.C. (2018). Continuous measurement of equilibrium equivalent radon/thoron concentration using time-integrated flow-mode grab sampler. *Acta Geophysica, 66*, 1267–1272. https://doi.org/10.1007/s11600-018-0163-9

26. Pivovarov, Yu.P., and Mikhalev, V.P. (2004). *Radiation ecology*. Moscow, Russian Federation: Akademiya.

27. Prister, B.S., Vinogradskaya, V.D., Lev, T.D., Talerko, M.M., Garger, E.K., Onishi, Y., and Tischenko, O.G. (2018). Preventive radioecological assessment of territory for optimization of monitoring and countermeasures after radiation accidents. *Journal of Environmental Radioactivity*, *184–185*, 140-151

28. Rabi, R., Oufni, L., and Amrane, M. (2017). Modeling of indoor ^{222}Rn distribution in ventilated room and resulting radiation doses measured in the respiratory tract. *Journal of Radiation Research and Applied Sciences*, *10*(3), 273-282.

29. Rabinskii, L.N., and Tushavina, O.V. (2019). Composite Heat Shields in Intense Energy Fluxes with Diffusion. *Russian Engineering Research*, *39*(9), 800-803.

30. Rabinskiy, L.N., and Tushavina, O.V. (2019a). Investigation of an elastic curvilinear cylindrical shell in the shape of a parabolic cylinder, taking into account thermal effects during laser sintering. *Asia Life Sciences*, *2*, 977-991.

31. Rabinskiy, L.N., and Tushavina, O.V. (2019b). Problems of land reclamation and heat protection of biological objects against contamination by the aviation and rocket launch site. *Journal of Environmental Management and Tourism*, *10*(5), 967-973.

32. Rabinskiy, L.N., Tushavina, O.V., and Formalev, V.F. (2019). Mathematical modeling of heat and mass transfer in shock layer on dimmed bodies at aerodynamic heating of aircraft. *Asia Life Sciences*, *2*, 897-911.

33. Rabinsky, L.N., and Kuznetsova, E.L. (2019). Simulation of residual thermal stresses in high-porous fibrous silicon nitride ceramics. *Powder Metallurgy and Metal Ceramics*, *57*(11-12), 663-669.

34. Renaud, J., Palmans, H., Sarfehnia, A., and Seuntjens, J. (2020). Absorbed dose calorimetry. *Physics in Medicine and Biology*, 65, Article number 05TR02

35. Saha, P., Uddin, M.H., and Reza, M.T. (2019). A steady-state equilibrium-based carbon dioxide gasification simulation model for hydrothermally carbonized cow manure. *Energy Conversion and Management*, *191*(1), 12-22.

36. Sean Hubar, J. (Ed.). (2017). *Fundamentals of oral and maxillofacial radiology*. Hoboken, New Jersey: John Wiley and Sons, Inc.

37. Shugurov, O., and Knyazyuk, A. (2018). Radiation situation in typical mining-processing agglomerations of the Dnepropetrovsk region. *Ecology and Noospherology, 29*(1), 8-12. https://doi.org/https://doi.org/10.15421/031802

38. Skvortsov, A.A., Kalenkov, S.G., and Koryachko, M.V. (2014). Phase transformations in metallization systems under conditions of nonstationary thermal action. *Technical Physics Letters, 40*(9), 787-790.

39. Starovoitov, É.I., and Leonenko, D.V. (2019). Effect of heat flow on the stressed state of a three-layer rod. *Journal of Engineering Physics and Thermophysics*, *92*(1), 60–72. DOI 10.1007/s10891-019-01907-9.

40. Starovoitov, E.I., Kubenko, V.D., and Tarlakovskii, D.V. (2009). Vibrations of circular sandwich plates connected with an elastic foundation. *Russian Aeronautics*, *52*(2), 151–157.

41. Taleyarkhan, R.P. (2020). Monitoring neutron radiation in extreme Gamma/X-Ray Radiation fields. *Sensors*, *20*, Article number 640.

42. Topchy, D.V. (2018). Organisational and technological measures for converting industrial areas within existing urban construction environments. *International Journal of Civil Engineering and Technology, 9*(7), 1975-1986.

43. Trotsenko, A.A., Zhuravleva, N.G., Aleksandrova, Ye.Yu., Yerokhova, N.V., and Udalova, O.A. (2019). Recommended practices for radioecological monitoring of the environment. *IOP Conference Series: Earth and Environmental Science*, *315*(5). Retrieved from https://iopscience.iop.org/article/10.1088/1755-1315/315/5/052077/meta.

44. Tushavina, O.V., Nadezhkina, E.V., Sorokin, A.E., Blinohvatov, A.A., and Zubkova, V.M. (2019). Study of the radiation situation in the city of Moscow. *Ecology of Urban Territories*, *3*, 73-76.

45. Umbetov, A., Kozhahmet, M., Sabitbekova, G., Amirov, M., Hamit, A., Alieva, G., Karimova, D., and Uspanova, V. (2017). Interference of coherent radiation in a crystalline two-component lens. *Far East Journal of Electronics and Communications, 17*(5), 923-939.

46. Umbetov, A.U., Umbetova, M.Z., Abildayev, G.M., Baizakova, S.S., Zhamalova, S.A., Konussova, A.B., and Dosmagulova, K.K. (2016). Transformation and interference of the laser radiation in composite crystal optical systems. *ARPN Journal of Engineering and Applied Sciences, 11*(19), 11561-11573.

47. Yakovlev, E.Y., Zykova, E.N., Zykov, S.B., Malkov, A.V., and Bazhenov, A.V. (2020). Heavy metals and radionuclides distribution and environmental risk assessment in soils of the Severodvinsk industrial district, NW Russia. *Environmental Earth Sciences*, *79*, Article number 218. Retrieved from https://doi.org/10.1007/s12665-020-08967-8

48. Yudaev, I., Stepanchuk, G., Kaun, O., Ukraitsev, M., and Ponamareva, N. (2019). Small-sized irradiation structures for intensive year-round cultivation of green vegetable crops. *IOP Conference Series: Earth and Environmental Science, 403*(1), 012084.

49. Zverev, V.L. (2010). *Fundamentals of ecology and problems of its development*. Moscow, Russian Federation: Ministry of Natural Resources and Ecology of the Russian Federation.

$$\varphi(z)=\varphi_0 e^{-\mu z} \quad \text{(Eq. 1)}$$

$$\mu=\sigma n_0=\sigma\frac{A_0\rho}{A}, \quad \text{(Eq. 2)}$$

$$I(z)=\varphi_0 t e^{-\mu z}. \quad \text{(Eq. 3)}$$

$$\theta_I=BI(z), \quad \text{(Eq. 4)}$$

$$I_0=\varphi_0 t \quad \text{(Eq. 5)}$$

$$\sigma_y=\sigma_{y0}\left[1+A\left(1-\exp\left(-\xi I_0\right)\right)^{1/2}\right], \quad \text{(Eq. 6)}$$

$$s'_{ij}=2G\text{э}'_{ij},\ \sigma'=K(3\varepsilon'-BI-\alpha\Delta T), \quad \text{(Eq. 7)}$$

$$s'_{ij}=2G\text{э}'_{ij}f'\left(\varepsilon'_u,I,a'_k\right), \quad \text{(Eq. 8)}$$

$$2\varepsilon'_{ij}=\mathcal{U}'_{i'j}+\mathcal{U}'_{j'i};\ \sigma'_{ij}l_j=R'_i \quad \text{(Eq. 9)}$$

$$\sigma'_{ij}l_j=R'_i\ to\ S_\sigma,\mathcal{U}'_i=\mathcal{U}'_{0i}\ to\ S_{\mathcal{U}}. \quad \text{(Eq. 10)}$$

$$I_1=\varphi t_1. \quad \text{(Eq. 11)}$$

$$z=c+h_1 \quad \text{(Eq. 12)}$$

$$s'^{(k)}_x=2G_k f^{(k)}(\varepsilon'^{(k)}_u,I)\text{э}'^{(k)}_x,\ \sigma'^{(k)}=K_k\left(3\varepsilon'^{(k)}-B_k I-\alpha_k\Delta T\right),\ \ (k=1,2,3),$$
$$s'^{(3)}_{xz}=2G_3 f'^{(3)}(\varepsilon^{(3)}_u,I)\text{э}'^{(3)}_{xz}, \quad \text{(Eq. 13)}$$

$$f'^{(k)}(\varepsilon'^{(k)}_u,I)=\begin{cases}1,\\ 1-\omega'^{(k)}(\varepsilon'^{(k)}_u,I),\end{cases}$$
$$\varepsilon'^{(k)}_u\le\varepsilon'^{(k)}_y(I), \quad \text{(Eq. 14)}$$
$$\varepsilon'^{(k)}_u>\varepsilon'^{(k)}_y(I);$$

$$\psi'^{(n)}(x)=C_2^{(n)}\operatorname{sh}(\beta x)+C_3^{(n)}\operatorname{ch}(\beta x)+$$
$$+\frac{1}{\beta}\left[\operatorname{sh}(\beta x)\int g'^{(n)}\operatorname{ch}(\beta x)\,dx-\operatorname{ch}(\beta x)\int g'^{(n)}\operatorname{sh}(\beta x)\,dx\right].$$
$$u'^{(n)}(x)=\gamma_3\psi'^{(n)}+\frac{1}{\alpha_2}\left[-a_4 L_2^{-1}\left(p'-p'^{(n-1)}_\omega\right)+a_7 L_3^{-1}\left(q'-q'^{(n-1)}_\omega\right)+\frac{a_7}{2}C_1^{(n)}x^2\right]+C_7^{(n)}x+C_8^{(n)}, \quad \text{(Eq. 15)}$$
$$w'^{(n)}(x)=\frac{1}{\alpha_2}\left[\alpha_1\int\psi'^{(n)}\,dx-a_7 L_3^{-1}\left(p'-p'^{(n-1)}_\omega\right)+a_1 L_4^{-1}\left(q'-q'^{(n-1)}_\omega\right)+\right.$$
$$\left.+\frac{1}{6}a_1 C_1^{(n)}x^3\right]+\frac{1}{2}C_4^{(n)}x^2+C_5^{(n)}x+C_6^{(n)}.$$

$$C_1^{(n)} = -\mathrm{L}_1^{-1}(q' - q_\omega'^{(n-1)})\big|_{x=l},\ C_3^{(n)} = \frac{1}{\beta}\int g'^{(n)}(x)\,\mathrm{sh}(\beta x)\,\mathrm{d}x\big|_{x=0},$$

$$C_2^{(n)} = \frac{1}{\beta}\left[\frac{\mathrm{ch}(\beta l)}{\mathrm{sh}(\beta l)}\left(\int g'^{(n)}\,\mathrm{sh}(\beta x)\,\mathrm{d}x\big|_{x=l} - \int g'^{(n)}\,\mathrm{sh}(\beta x)\,\mathrm{d}x\big|_{x=0}\right) - \int g'^{(n)}\,\mathrm{ch}(\beta x)\,\mathrm{d}x\big|_{x=l}\right],$$

$$C_4^{(n)} = \frac{a_7}{\alpha_2}\left[\mathrm{L}_1^{-1}(p' - p_\omega'^{(n-1)}) + \sum_{k=1}^{3}\left(B_k I_k + \alpha_\kappa \Delta T\right) K_k h_k\right]\Big|_{x=l} -$$

$$-\frac{a_1}{\alpha_2}\left(\mathrm{L}_2^{-1}(q' - q_\omega'^{(n-1)}) + \left(B_1 I_1 + \alpha_1 \Delta T\right) K_1 h_1\left(c + \frac{h_1}{2}\right) - \left(B_2 I_2 + \alpha_2 \Delta T\right) K_2 h_2\left(c + \frac{h_2}{2}\right)\right)\Big|_{x=l} - \frac{a_1}{\alpha_2} C_1^{(n)} l,$$

$$C_5^{(n)} = \frac{a_7}{\alpha_2}\mathrm{L}_2^{-1}\left(p' - p_\omega'^{(n-1)}\right)\big|_{x=0} - \frac{a_1}{\alpha_2}\mathrm{L}_3^{-1}\left(q' - q_\omega'^{(n-1)}\right)\big|_{x=0},$$

$$C_6^{(n)} = \frac{a_7}{\alpha_2}\mathrm{L}_3^{-1}(p' - p_\omega'^{(n-1)})\big|_{x=0} - \frac{a_1}{\alpha_2}\mathrm{L}_4^{-1}(q' - q_\omega'^{(n-1)})\big|_{x=0} - \frac{\alpha_1}{\alpha_2}\int \psi'^{(n)}\,\mathrm{d}x\big|_{x=0},$$

$$C_7^{(n)} = \frac{a_4}{\alpha_2}\left[\mathrm{L}_1^{-1}(p' - p_\omega'^{(n-1)})\big|_{x=l} + \sum_{k=1}^{3}\left(B_k I_k + \alpha_\kappa \Delta T\right) K_k h_{kk}\right] -$$

$$-\frac{a_7}{\alpha_2}\left(\mathrm{L}_2^{-1}(q' - q_\omega'^{(n-1)})\big|_{x=l} + \left(B_1 I_1 + \alpha_1 \Delta T\right) K_1 h_1\left(c + \frac{h_1}{2}\right) - \left(B_2 I_2 + \alpha_2 \Delta T\right) K_2 h_2\left(c + \frac{h_2}{2}\right) - C_1^{(n)} l\right),$$

$$C_8^{(n)} = \frac{a_4}{\alpha_2}\mathrm{L}_2^{-1}(p' - p_\omega'^{(n-1)})\big|_{x=0} - \frac{a_7}{\alpha_2}\mathrm{L}_3^{-1}(q' - q_\omega'^{(n-1)})\big|_{x=0}. \qquad \text{(Eq. 16)}$$

$$\psi^{(n)*}(x) = C_2^{(n)*}\,\mathrm{sh}(\beta x) + C_3^{(n)*}\,\mathrm{ch}(\beta x) +$$

$$+\frac{1}{\beta}\left[\mathrm{sh}(\beta x)\int g^{(n)*}\,\mathrm{ch}(\beta x)\,\mathrm{d}x - \mathrm{ch}(\beta x)\int g^{(n)*}\,\mathrm{sh}(\beta x)\,\mathrm{d}x\right].$$

$$u^{(n)*}(x) = \gamma_3 \psi^{(n)*} + \frac{1}{\alpha_2}\left[-a_4\,\mathrm{L}_2^{-1}\left(p^* - p_\omega^{(n-1)*}\right) + a_7\,\mathrm{L}_3^{-1}\left(q - q_\omega^{(n-1)*}\right) + \frac{a_7}{2} C_1^{(n)*} x^2\right] +$$

$$+C_7^{(n)*} x + C_8^{(n)*}, \qquad \text{(Eq. 17)}$$

$$w^{(n)*}(x) = \frac{1}{\alpha_2}\left[\alpha_1 \int \psi^{(n)*}\,\mathrm{d}x - a_7\,\mathrm{L}_3^{-1}\left(p^* - p_\omega^{(n-1)*}\right) + a_1\,\mathrm{L}_4^{-1}\left(q^* - q_\omega^{(n-1)*}\right) +\right.$$

$$\left.+\frac{1}{6} a_1 C_1^{(n)*} x^3\right] + \frac{1}{2} C_4^{(n)*} x^2 + C_5^{(n)*} x + C_6^{(n)*}.$$

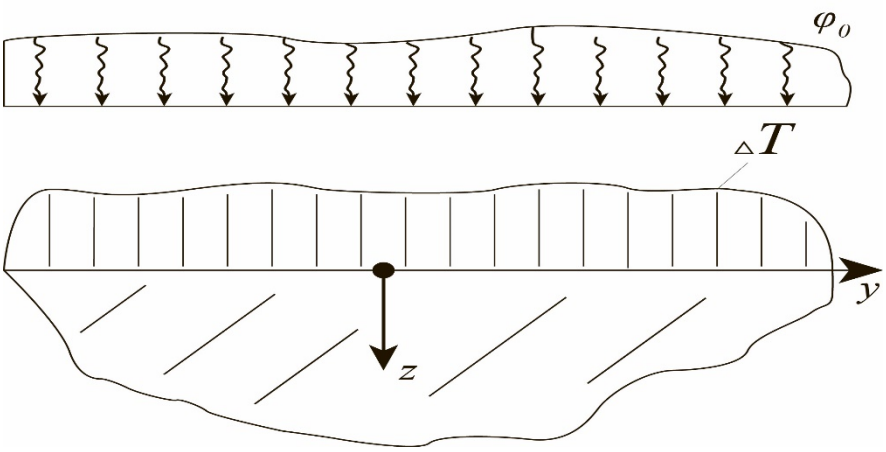

Figure 1. *Diagram of loading on an isotropic body*

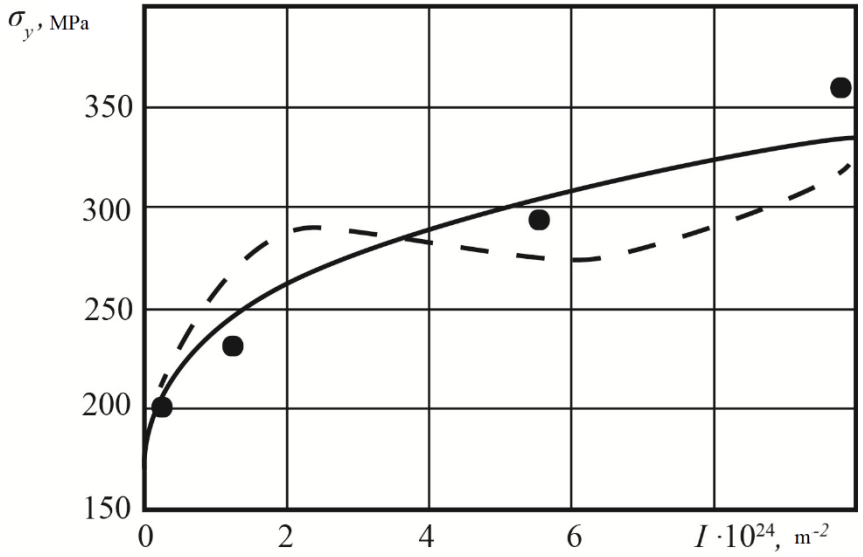

Figure 2. *The dependence of stress on the neutron flux magnitude*

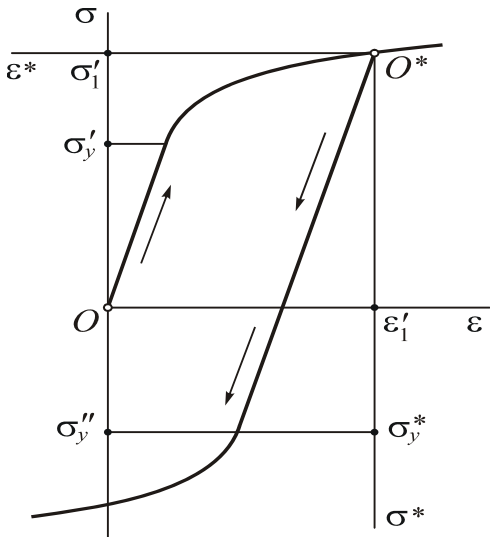

Figure 3. *The diagram of stress-strain and unloading*

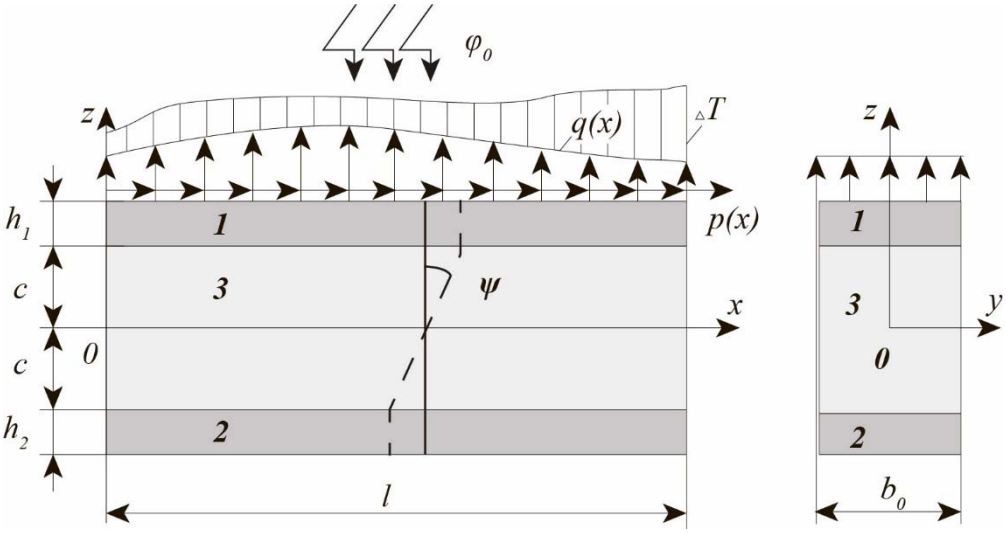

Figure 4. *The load on the three-layer beam*

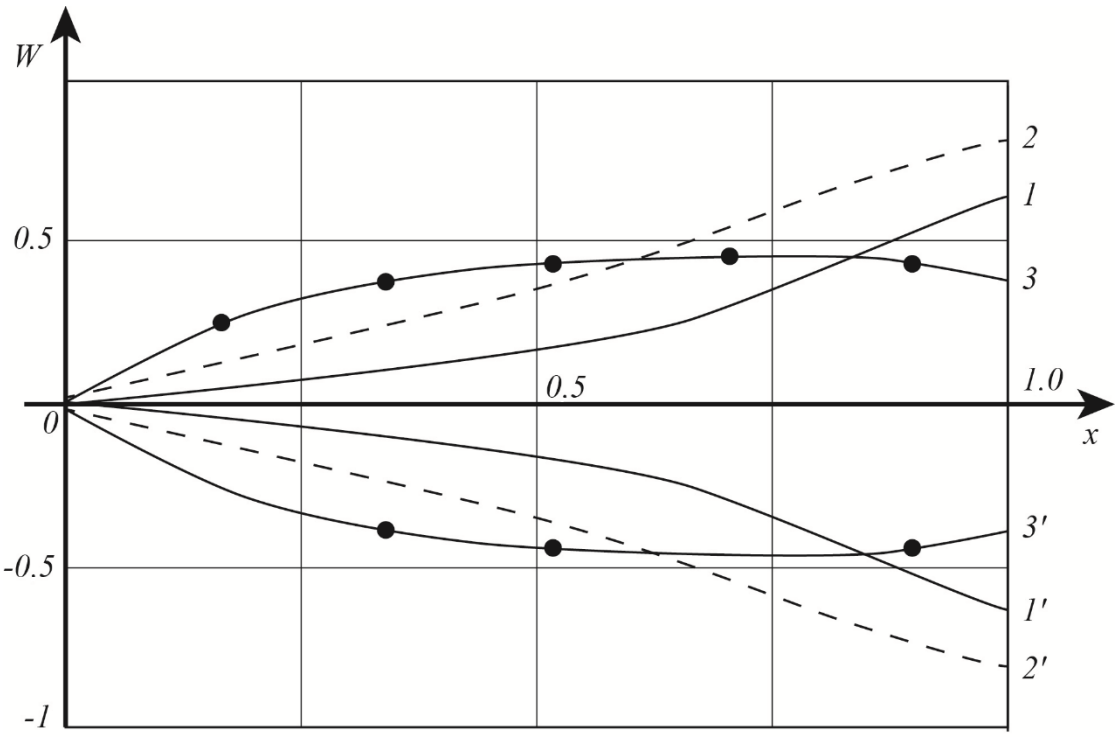

Figure 5. *The distribution of deflection along the axis of a three-layer rod*